LIMNOLOGY
AND
OCEANOGRAPHY

September 2006
Volume 51
Number 5

*Limnol. Oceanogr.*, 51(5), 2006, 1941–1955


# Inertial oscillations and related internal beat pulsations and surges in Lakes Michigan and Ontario

*C. H. Mortimer*[1]
Center for Great Lakes Studies, University of Wisconsin-Milwaukee, P.O. Box 413, Milwaukee, Wisconsin 53201

*Abstract*

Records of water temperature, current, and wind, made during campaigns on Lakes Michigan 1963 and Ontario 1972, are searched for inertial responses to wind action: (i) circle-tracking currents; and (ii) isotherm-depth undulations, i.e., long internal wave manifestations of forcing by wind. With stratification absent in winter, only response (i) is seen (and then only rarely) with periods very close to the local inertial period, $T_{in}$. After whole-basin stratification is complete, both responses (i) and (ii) occur frequently, as internal Kelvin waves (shore-trapped and not further treated here) and cross-basin Poincaré internal seiche modes. Mode periods range between 1% and 15% less than $T_{in}$, depending on which of the here-modeled modes have responded and on differences between modes in their partitioning of kinetic and potential energy. When, in both lakes, short-duration wind impulses were followed by a week or more of relative calm, Poincaré mode combinations produced beat pulsations in both responses (i) and (ii), diagnostic features of which sometimes permitted participating modes to be identified. At a nearshore downwelled front in Lake Ontario, another type of poststorm adjustment was seen. Periodically released from the front, internal surges migrated across the basin through fields of inertially rotating, response (i) currents.

Long internal waves, responding to wind action and the earth's rotation in basins of the size considered here, fall into two classes: shore-hugging Kelvin waves of very long period; and Poincaré wave modes, occupying the whole basin and displaying periods close to but always less than $T_{in}$, the local inertial period. Features of these two wave classes were illustrated for a (two-layered) flat-bottomed model of Lake Ontario (Schwab 1977, Kelvin period 598 h, Poincaré period 17.35 h) and for two-layered channels in Mortimer (2004). There it was shown that internal Kelvin wave amplitude, maximal at the shore, falls to about 2% at a distance of four internal Rossby (1937, 1938) radii (≈16 km) offshore in Lake Michigan. Kelvin waves are therefore restricted to within the nearshore hatched areas in the Fig. 2B model and are not further treated here.

Such neglect is not possible in lakes one size-order smaller than Michigan, for example Lakes Kinneret (Antenucci and Imberger 2001, 2003) and Geneva (Lemmin et al. 2005). In those basins, approximately two Rossby radii wide for internal waves, both Kelvin and Pointcaré waves occupy the whole basins.

The treatment here of near-inertial motions, principally internal Poincaré modes, is largely descriptive; but references to more advanced models and analytical theory are given in the summary, which also poses further questions.

When motion of a water mass is governed by inertia alone, its track (as seen by an observer on the rotating earth) is not a straight line, but one that veers to the right in the northern hemisphere. In a large lake or ocean, remote from shore, the observer sees that track as an *inertial circle*, completed in an *inertial period* $12\ (\sin \Phi)^{-1}$ h at latitude $\Phi^{\circ}$. In this paper, that period is designated as $T_{in}$. It is 17.4 and 18.0 h, respectively, at the north and south ends of Lake Michigan. Radii of inertial circles are proportional to current speed. At 10 cm $s^{-1}$, at the latitudes here considered, the radius is close to 1 km. Inertial circling is often combined with other currents, which vary little or not at all in direction. The combined current track is, then, "looping," "waltzing," or "meandering," as commonly seen in both lakes.

Such loops were conspicuous in the track of a drifter buoy, followed at 3-m depth for 19 d by McCormick et al. (1991) in a 50 × 35 km area centered in the southern basin

[1] Corresponding author (abrooks@uwm.edu).

*Acknowledgments*

I appreciate the assistance given to me, in preparation of this paper during my retirement, by colleagues at the University of Wisconsin–Milwaukee: Arthur Brooks, Harvey Bootsma, Thomas Hansen, and Peter Watson-Boone. Phyllis Shaw typed the final manuscript. I also thank two anonymous reviewers for their comments, corrections, and efforts to bring me up to date.

of Lake Michigan. That track, illustrated and analyzed in Mortimer (2004), displayed 26 regular 17-h inertial loops superimposed on wider meanderings. Those were compared with wind data from a nearby buoy, operated by the U.S. National Oceanic and Atmospheric Administration (NOAA). Interactions of inertial circling with other current systems are not further pursued in this paper, which only examines variations in periodicities of inertial and near-inertial responses, observed in current and water temperature records obtained during two major campaigns on the lakes. Similar responses had first been detected (Mortimer 1963, 2004) in temperature records from municipal water intakes around Lake Michigan.

Deployment of wind, current, and temperature recorders in the Laurentian Great Lakes occurred, first (1962–1964) in Lake Michigan, and later in other lakes. For Lake Michigan, a description of methods and a few results appeared in a substantial report (FWPCA 1967). Prompted by pollution concerns, that campaign was initially managed by the U.S. Public Health Service with J. L. Verber in charge. In 1963, thirty-four recording stations, each with instruments at several depths, were deployed to cover the whole lake; but regrettably that monumental effort was not matched by later reporting and analysis.

The publication list is small: FWPCA (1967); preliminary descriptions of the project and features of rotating currents (Verber 1963, 1964, 1966); Malone's spectral analyses of currents (1968); and Allender's (1977) comparison of observed currents with those predicted by then-available models, which "did not compare well."

Previous analysis of long series of water temperature records from municipal intakes around the shores of Lake Michigan led me to predict (Mortimer 1963) that the FWPCA offshore recorders would include signals from internal rotation-influenced waves with near-inertial periods. So it turned out, although some "generalized current" illustrations in that paper proved to be erroneous.

During a 1962–1963 visit to the University of Wisconsin–Madison, I supplemented the FWPCA recordings with a set of repeated cross-lake isotherm-depth surveys with railroad ferries on their regular Milwaukee to Muskegon crossings. During July and August 1963, eighty transects were completed with bathythermograph casts every 6 min (2 km). The findings, illustrated in Mortimer (1968, 2004) and discussed here in connection with Figs. 3 to 6, revealed large poststorm cross-basin undulations of thermocline depth. These were dominated by odd-numbered modes of internal (Poincaré) cross-basin seiches (Poincaré 1910), with a common midlake node at 66 km east of Milwaukee (Fig. 3).

The FWPCA 1963 records, here searched for inertial episodes, came from three sources: (i) FWPCA, (1967); (ii) unpublished computer prints of wind, current, and temperature records provided by the Chicago Office, U.S. Environmental Protection Agency (successor to FWPCA); and (iii), (with permission) Malone's (1972) unpublished thesis.

*Estimation of periods—the method.* For each selected oscillation episode, typically comprising eight or more cycles, a mean oscillation (MO) period was estimated, to $\pm 0.1$ h, by eye with the help of a 10-point divider. That estimated period, which will be referred to hereafter as the MO period, was marked (for each episode) by a set of equally spaced symbols.

Figure 1B and C illustrate the unusual method adopted by FWPCA (by Mehr 1965) for plotting the 1963 records of speed and direction of current and wind. For each 2-h interval, only the extreme readings (e.g., speed maxima, minima, and direction excursions) were retained by FWPCA and joined by vertical lines in all their plots. The midpoints of those lines, plotted here in later figures, are (it should be noted) rough approximations only to mean values; but they suffice to follow events on the time scales relevant here.

In the winter example (Fig. 1B), the MO period (17.5 h) was indistinguishable from the local inertial period $T_{in}$ (17.55 h). The same held true for the infrequent winter episodes of current oscillation found by Marmorino (1978) in Lake Ontario, to be described later. In both lakes, during whole-basin stratification in summer, oscillation episodes were frequent and included temperature as well as current responses. MO periods were then distinctly less than $T_{in}$; and (as explained later) the MO period for the temperature oscillation was often less than that of the accompanying current oscillation. In Fig. 1C, a summer example, the current and temperature MO periods are, respectively, 2% and 6% less than $T_{in}$. It is here noted that, in the search through summer inertial episodes, only one example has been recorded (Verber 1964) in which the MO period was indistinguishable from $T_{in}$. That was a July 1963 current record from Sta. 1, which Fig. 1A places at the southern extremity of the basin.

To minimize end effects, attention here is confined to stations in the middle reaches of Lakes Michigan and Ontario, where the cross-basin internal seiche modes, introduced later, come into play.

*The cross-basin internal (Poincaré) seiche modes, modeled*—The season of whole-basin stratification in summer and fall is characterized by the presence of a thermocline, in which the density gradient suppresses turbulence and therefore internal friction. Consequently, the layers above and below the thermocline can slide over each other with relative ease, when displaced by wind action on the water surface. When, in the northern hemisphere, wind blows along the basin, that displacement, coupled with the earth's rotation, leads to (i) thermocline downwelling near the shore lying to the right of the wind track and (ii) to nearshore upwelling along the opposite shore (hatched areas D and U in Fig. 2B; *see also Fig. 3*). The responses, to that wind-produced cross-basin asymmetry in the distribution of potential energy, are shore-trapped internal Kelvin waves and internal Poincaré seiches with odd-numbered modes preferred (Fig. 2B). Associated Poincaré currents rotate clockwise, as shown for the lower layer only in Fig. 2A. Upper layer currents, also clockwise-rotating, are 180° out of phase with those in the lower layer.

Figure 2 belongs to the simplest class of uniform-depth channel models with two homogeneous fluid layers, which I

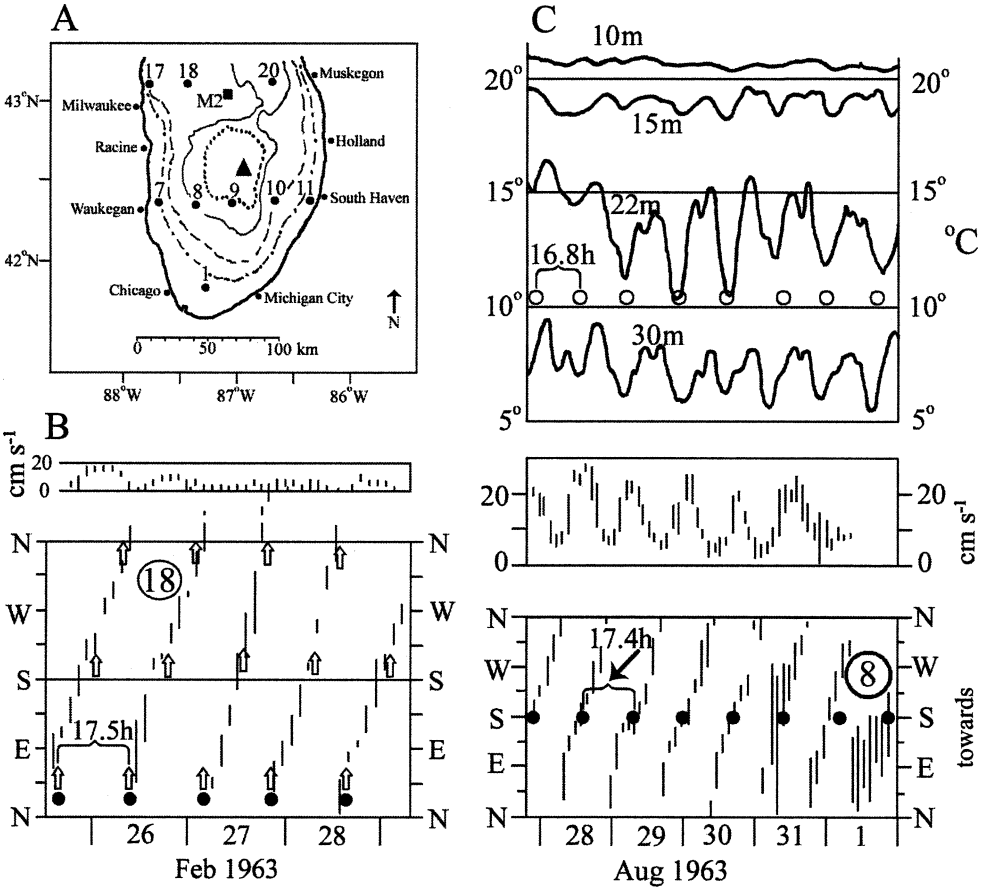


Fig. 1. (A) Locations in southern Lake Michigan of selected 1963 moorings (FWPCA 1967) and anchor station M2 (Mortimer 2004) with depth contours: 40, 70, 100, 130 m and maximum depth (167 m) marked by triangle. (B, C) Representative 1963 records, as plotted by FWPCA; (B) in winter (adapted from Verber 1963); (C) in summer (currents from Malone 1968; temperatures from FWPCA 1967). Equally spaced symbols indicate the mean oscillation (MO) periods, estimated as described in text.

used (Mortimer 2004) to illustrate some properties of rotation-affected internal Kelvin and Poincaré waves. More realistic models (circular and elliptical rotating basins) were developed by Antenucci and Imberger (2001, 2003). (For a comprehensive theoretical treatment of such waves, in the context of tidal motions, *see* Platzman 1971, 1972, and Gill 1982.)

As a first step, a governing variable in the Fig. 2B model must be calculated for the case in which rotation influence is zero or negligible, as in small lakes. That "no-rotation phase speed," or celerity, $c_i$, is the speed at which long internal waves would travel on the thermocline interface, if the channel were not rotating. Then,

$$c_i^2 = g\,(\rho_2 - \rho_1)\,h_1 h_2\,[\rho_2(h_1 + h_2)]^{-1} \qquad (1)$$

determined by the respective layer densities and thicknesses ($\rho_1$, $\rho_2$, $h_1$, $h_2$) and $g$, the acceleration of gravity.

The Lake Michigan episode illustrated in Fig. 3 and the repeated cross-basin isotherm depth surveys in Mortimer (2004) indicate the approximate thickness of $h_1$ and $h_2$ to be 27 and 45 m and the mean layer temperatures to be 16°C and 4.5°C, respectively. This corresponds to $(\rho_2 - \rho_1) = 1.027 \times 10^{-3}$ g cm$^{-3}$ and a $c_i$ value of 0.41 m s$^{-1}$. The Lake Ontario episode in Figs. 12 and 13 and the temperature transect Fig. 14 show approximate layer thicknesses for $h_1$ and $h_2$ of 11 and 75 m, with mean layer temperatures again at 16°C and 4.5°C, yielding $c_i = 0.29$ m s$^{-1}$. Therefore, for the mode properties calculated in Tables 1 and 2, the Lake Michigan and Ontario approximate celerities $c_i$ are respectively taken as 0.4 and 0.3 m s$^{-1}$.

The odd-numbered internal cross-basin modes 1, 3, and 5 are illustrated with their respective nodal locations in the Fig. 2B channel of width $w$. Their amplitudes and phases, there initially equal, will change as the oscillations progress. Their wavelengths are, respectively, $2w$; $2w\ (3)^{-1}$; and $2w\ (5)^{-1}$. The corresponding rotation-absent periods are $2w\ (c_i)^{-1}$; $2w\ (3c_i)^{-1}$; and $2w\ (5c_i)^{-1}$. These are sometimes called *Merian periods* (appropriate for small lakes), here designated as $T_m$. For clarity in later discussion, it is convenient to refer to $c_i$ as the *Merian celerity* and to the internal seiche modes (when not rotating) as *Merian modes*.

Influenced by rotation, the picture changes radically. The Merian modes become Poincaré modes with periods $T_p$ given (in Mortimer 2004) as $T_p^{-2} = T_{in}^{-2} + (1 + \tau^2)\,T_m^{-2}$,

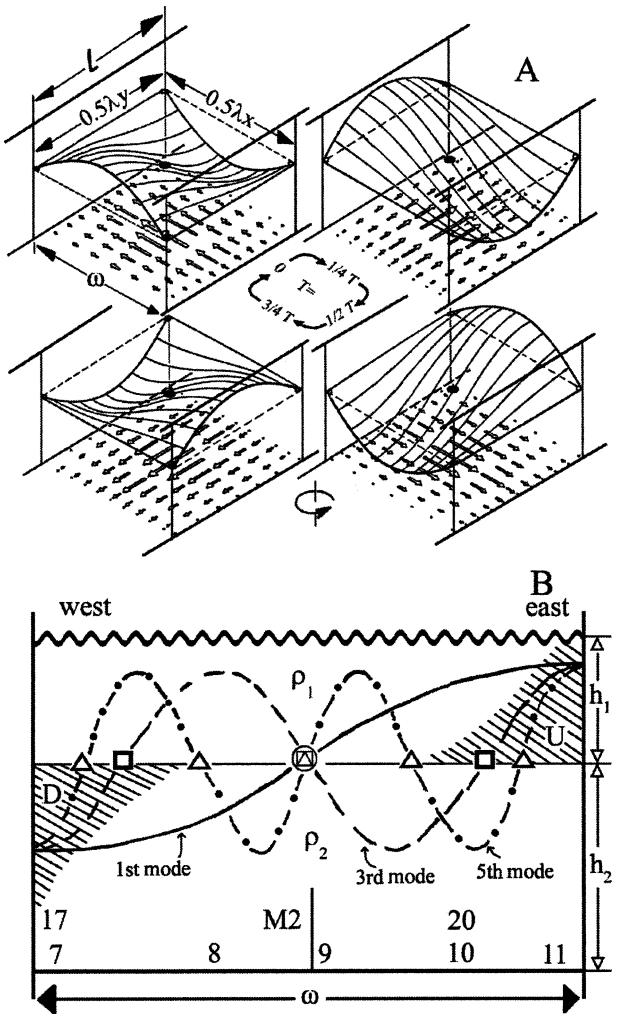


Fig. 2. Internal Poincaré wave modes in the two-layered rectangular rotating model channel described in text. (A) Quarter-cycle stages of a first-mode wave in a short section of a longer channel of width $w$. (B) Cross section of the channel, with mode numbers 1, 3, and 5 (initially of equal amplitude and in phase) on the interface between layers $h_1$ and $h_2$. Also shown (hatched) are wind-generated upwelling (U) and downwelling (D) near-shore distortions of the interface. Nodal positions are marked by symbols. Numbers mark Lake Michigan recording station positions, approximately spaced as in the lake (Fig. 1A).

in which $T_{in}$ and $T_m$ were defined earlier and $\tau$ is the ratio of cross-channel to along-channel wavelength, $\lambda_x\,(\lambda_y)^{-1}$. This follows from the dispersion relationship set out in Platzman (1971). $\lambda_y$ is equal to $\lambda_x$ in Fig. 2A, but is much longer than $\lambda_x$ in the lakes considered here. For example, in Schwab's (1977) numerical model of a two-layered flat-bottomed Lake Ontario, $\tau^2$ for the first Poincaré mode was 0.056 and is neglected here, leaving

$$T_p^{-2} = T_{in}^{-2} + T_m^{-2} \qquad (2)$$

for the calculation of $T_p$ in Table 1. It is evident that, as channel width $w$ and therefore $T_m$ increase, $T_p$ approaches, but never exceeds $T_{in}$. Periods $T_p$ for cross-basin modes 1, 3, 5, and 7 are calculated for two latitudes in Lake Michigan ($w$ = 120 km) and for one latitude in Lake Ontario ($w$ = 70 km) corresponding to locations of stations, records from which are now examined.

The fit between the odd-numbered mode structure, modeled in Fig. 2B and observed in Lake Michigan, is illustrated in Fig. 3. Isotherm depths are shown for a west-to-east ferry crossing with the 10°C (midthermocline) isotherm emphasized as a bold line. That isotherm, on the return east-to-west crossing, is shown dotted. At 12.4-km intervals along the base of Fig. 3 are noted the hours that had elapsed between the two crossings. Evident are: persistent upwelling/downwelling of the thermocline within 20 km of each shore, within which Kelvin waves are trapped. Elsewhere, the transect was occupied by a standing wave structure with five nodes (triangles), of which 1 and 5 were obscured by nearshore upwelling/downwelling and by Kelvin wave action. Only the midlake node 3 was clearly identified. This was because: (i) the ferry passage interval at that point was close an inertial half-cycle (8 h); and (ii) even-numbered modes were inconspicuous or absent. The midlake node was therefore common to all odd-numbered modes.

*Inertial oscillatory episodes in Lake Michigan, summer and fall 1963*—After a quiescent interval in late July, FWCPA Sta. 18 recorded a short, strong wind impulse on 02 August, which set a regular series of current and temperature oscillations in motion at Sta. 20 (Fig. 4B, C). Those oscillations lasted, with little diminution in amplitude, for 9 d until disturbed by a storm on 12–13 August. The MO periods of current and temperature oscillations (17.4 and 16.9 h, respectively) were 1% and 4% less than $T_{in}$ (17.55 h) and close to the periods ascribed to model cross-channel modes 1 and 3 in Table 1.

That difference in MO period between contemporary current and temperature oscillations, seen in many inertial response episodes, is explained (in the development of fig. 6-15 in Mortimer 2004) by the relationship between a mode's wave length and its partition of total energy into kinetic and potential parts. For example, the percentages of kinetic (current) energy contained in the energy totals of the Lake Michigan Poincaré modes 1, 3, 5 and 7 (periods listed in Table 1) are, respectively, 99.4%, 95.4%, 87.5%, and 77.8%. Therefore, when two modes are excited together, with equal or near-equal amplitudes, the mode with the lower number (and longest period) will be expressed more strongly in (kinetic) current circling than in (potential) thermocline undulation.

Figure 4 is also an example of the general observation that short wind impulses, lasting for less than half an inertial period, are often more effective generators of inertial response than are winds of equal strength lasting longer. This was demonstrated, for ocean episodes, by Pollard and Millard (1970). A unidirectional wind impulse will drive the circling current during the first half of the inertial cycle, but will brake it during the second half.

The strongest inertial response occurs when the wind direction is also rotating clockwise with the current. In general, therefore, inertial response strength and the

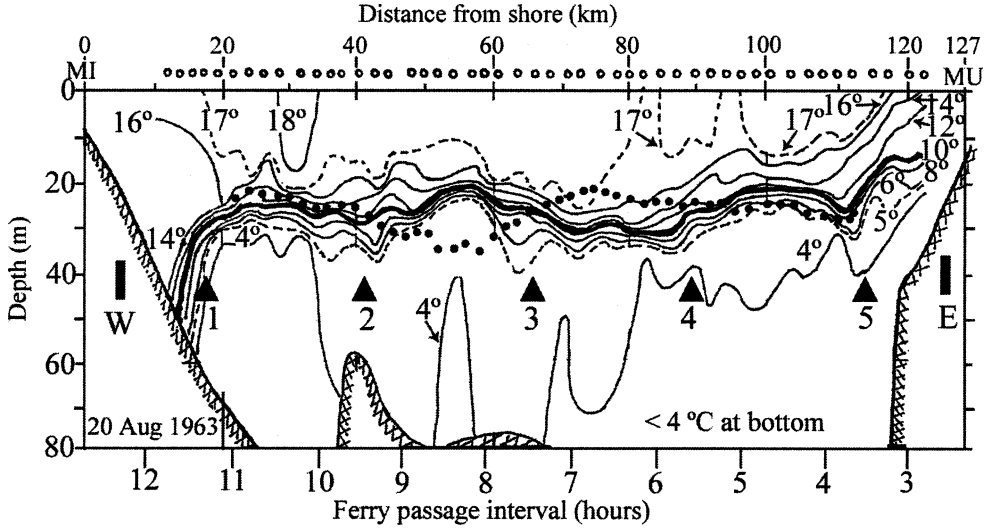


Fig. 3. Isotherm depths during 20 August 1963 ferry runs, Milwaukee to Muskegon and back. For the outward run, isotherms, 4° to 18° are shown (at 2°C intervals with 5° and 17°) and with 10°C emphasized (thick line). For the return run, only the 10°C isotherm is shown (dotted). Open circles along the top indicate locations of bathythermograph casts. Triangles 1 to 5 indicate estimated locations of nodes of the fifth Poincaré mode. Hours, marked along the bottom, indicate time elapsed at those locations between outward and return ferry passages.

selection of which internal Poincaré modes are excited are determined, not only by the strength of the wind, but also by its duration and curl.

Temperature oscillations in Lake Michigan were usually nearly in phase at all depths, indicating a simple vertical structure of the internal wave. But that was not always the case, for example in Fig. 4C (Sta. 20). From 04 to 07 August, temperature oscillations at 15- and 22-m depths were nearly in phase, but about one-quarter cycle out of phase with the 10-m oscillation. After the very short southgoing wind impulse of 07 August, the phase difference between the 15- and 22-m records shifted by about one-quarter cycle.

Although Sta. 17 (Fig. 4D, water depth 22 m) was only 4 km from the west shore and was separated by 90 km from Sta. 20 on the opposite side of the basin, a 16.9 h oscillation in temperature was observed at 15-m depth at both stations from 04 to 07 August. Those oscillations were nearly out of phase, suggesting that the whole cross-section was oscillating. Downwelling at Sta. 17 (and at the nearby Milwaukee water intake), produced by the southgoing wind impulse on 09 August, obliterated the cross-basin oscillation at Sta. 17; but it persisted at Sta. 20 until destroyed by the upwelling produced there by the 13 August storm.

*Half-inertial periodicity appearing in internal Poincaré wave records when the amplitude becomes large*—When inertial oscillation amplitudes become large, small-amplitude (linear) theory no longer applies; and nonlinear features appear. This was demonstrated (Mortimer 2004) by current and isotherm-depth measurements at midlake anchor station M2 (Fig. 1A) covering 3-d intervals: (a) before; and (b) after the 02 August wind impulse. Records during (a) displayed Poincaré waves of near-inertial period, of small amplitude and sinusoidal form. During (b), wave amplitude had tripled and the wavefront had steepened (triangles in Fig. 5A). Also a component (marked by open squares in Fig. 5A) had appeared with a half-inertial period. Similar half-inertial components, accompanying large Poincaré wave amplitudes, often appeared as secondary peaks in spectra of summer currents in Lake Michigan (Malone 1968) and in Lake Ontario (fig. 5B from Marmorino and Mortimer 1978).

Table 1. Periods, $T_m$ and $T_p$, defined in the text, of internal cross-channel Poincaré modes 1, 3, 5, and 7, in model 2B, calculated for two rows of recording stations in Lake Michigan (channel width $w$ = 120 km) and one row in Lake Ontario ($w$ = 70 km), with $c_i$ settings of 0.4 m s$^{-1}$ for Lake Michigan and 0.3 m s$^{-1}$ for Lake Ontario.

| | | Inertial period (h) | Mode numbers and periods (h) | | | | | | | |
|---|---|---|---|---|---|---|---|---|---|---|
| | | | No. 1 | | No. 3 | | No. 5 | | No. 7 | |
| Lake Michigan Sta. | Latitude (°N) | $T_{in}$ | $T_m$ | $T_p$ | $T_m$ | $T_p$ | $T_m$ | $T_p$ | $T_m$ | $T_p$ |
| 17, M2, 20 | 43°08′ | 17.55 | 167 | 17.4 | 56 | 16.7 | 33 | 15.5 | 24 | 14.1 |
| 7, 8, 11 | 42°23′ | 17.80 | 167 | 17.7 | 56 | 17.0 | 33 | 15.7 | 24 | 14.2 |
| Ontario 9, 10, 16 | 43°40′ | 17.38 | 130 | 17.2 | 43 | 16.1 | 26 | 14.4 | 19 | 12.7 |

Table 2. Beat periods and mean oscillation (MO) periods resulting from paired combinations of equiamplitude internal Poincaré modes of respective periods a and b (*see Table 1*) for Lake Michigan Sta. 8; Lake Ontario Sta. 10; and for the beat pulsation model illustrated in Fig. 6C.

| Mode pairs | Mode periods, $T_p$ in Table 1 (h) $a$ $b$ | MO periods (h), 0.5 $(a + b)$ | Beat periods (d), $ab/(24(a - b))$ |
|---|---|---|---|
| Lake Michigan | | | |
| 1 and 3 | 17.7 17.0 | 17.4 | 17.9 |
| 1 and 5 | 17.7 15.7 | 16.7 | 5.8 |
| 1 and 7 | 17.7 14.2 | 16.0 | 3.0 |
| 3 and 5 | 17.0 15.7 | 16.4 | 8.6 |
| 3 and 7 | 17.0 14.2 | 15.6 | 3.6 |
| 5 and 7 | 15.7 14.2 | 15.0 | 6.2 |
| Fig. 6C model | 17.4 15.8 | 16.6 | 7.2 |
| Lake Ontario | | | |
| 1 and 3 | 17.2 16.1 | 16.7 | 10.5 |
| 1 and 5 | 17.2 14.4 | 15.8 | 3.7 |
| 3 and 5 | 16.1 14.4 | 15.3 | 5.7* |

* The beat periods for other Lake Ontario mode pair are less than 2.5 d.

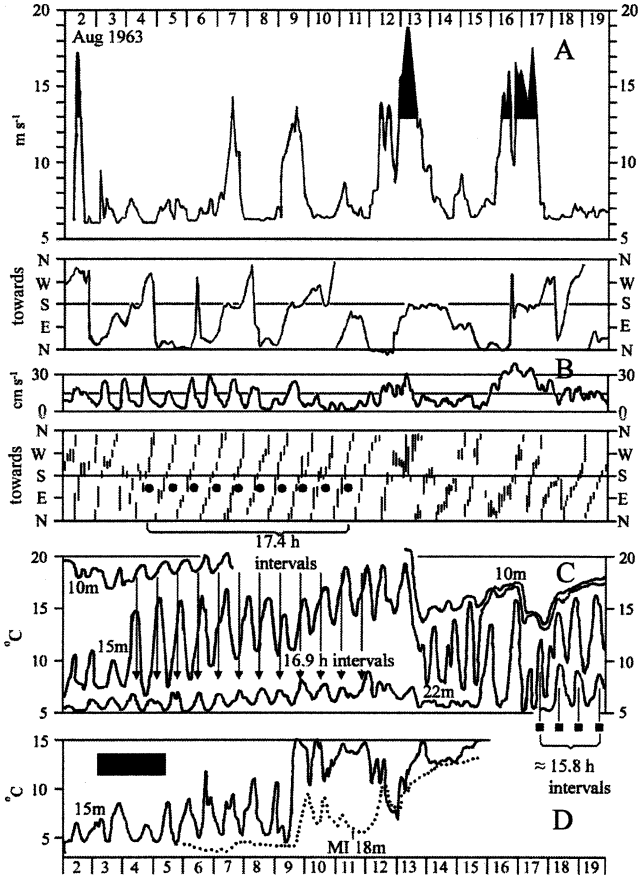


Fig. 4. Lake Michigan, 02 to 19 August 1963, here adapted from figures in FWPCA (1967) and unpublished FWPCA records. (A) Wind speed and direction at Sta. 18, plotted on a linear scale from the midpoints of FWPCA (unpublished) 2-h envelopes, as is also (B) current speed and direction at 60-m depth at Sta. 20; (C) temperature (°C) at 10-, 15-, and 22-m depth at Sta. 20 (from FWPCA 1967); and (D) temperature (°C) at 15-m depth at Sta. 17 and (dotted line) at nearby Milwaukee water intake (MI 18-m depth). Equally spaced symbols mark estimates of mean oscillation (MO) periods during episodes of inertial response, as described in the text. This figure continues in Fig. 6. The black bar in (D) marks the duration of Fig. 5A. The peak winds in this and later figures are blackened for emphasis.

*Beat interactions when two modes oscillate together*—With a 3-d overlap, Fig. 6 is a continuation of Fig. 4 and starts with the storm on 17 August. During the 2 d (18 and 19 August) following the storm, the temperature record from Sta. 20 (Fig. 4C) showed the beginnings of an oscillation of MO period 15.8 h, close to that calculated for the fifth Lake Michigan mode in Table 1. That storm was followed by 1 week of calm weather and weak winds, followed in turn by short wind pulses on 23 and 28 August. During the calm spell, cross-lake isotherm-depth surveys (19–22 August, Mortimer 2004) revealed a combined response of the first and fifth Poincaré cross-basin modes with the fifth dominant. Conspicuous was a common midlake node 66 km east of Milwaukee (Fig. 3).

Continuing into the "calm" spell during the 10 d of weak winds following the 17 August storms, temperature oscillations at Sta. 8 (Fig. 6B) displayed a pulsating pattern with minima (M) spaced about 7 d apart. The individual oscillations, the amplitudes of which rose to a maximum and faded away, showed regular MO periods of 16.6 h. This pulsating pattern resembles a *beat pattern*, well known in acoustics, in which two tones of similar amplitude but slightly differing pitch (corresponding periods $a$ and $b$) sound together to produce a pulsating tone of intermediate pitch, corresponding to an MO period of 0.5 $(a + b)$.

The longer intervals between pulse minima (the *beat period*) is $ab\ (a-b)^{-1}$. If periods $a$ and $b$ are known and the amplitudes are equal or nearly so, it is therefore possible to estimate the MO and beat periods for any paired combination of oscillations, including the pairs of modes listed in Table 2, for six Lake Michigan mode pairs; three Lake Ontario mode pairs; and one for the Fig. 6C model. That model consisted of two of equal-amplitude sine waves (period $a$ = 17.4 h, $b$ = 15.8 h) and was constructed to fit the MO period (16.6 h) observed in Fig. 6B and to test whether the pulsating 6B record was, in fact, a beat. The component periods of the Fig. 6C model (17.4 and 15.5 h) are closest to those assigned to Lake Michigan modes 1 and 5 in Table 1. That combination was also seen in the 18 to 23 August 1963 cross-lake surveys of thermocline depth (Mortimer 2004), but with the fifth mode contribution larger than that of the first mode.

The beat interpretation is supported, not only by similarities in the outline form between 6B and 6C, but, significantly, also by the fact that the individual oscillations (MO period 16.6 h in Fig. 6B and Fig. 6C) both change phase by one half cycle on passing through each minimum M. That phase change proves to be a useful diagnostic tool for the identification of beat patterns.

The beat pattern in Fig. 6B disappeared after the wind impulse on 28 August. At Sta. 9 (Fig. 6D), the temperature record did not show a beat pattern; and the large amplitude

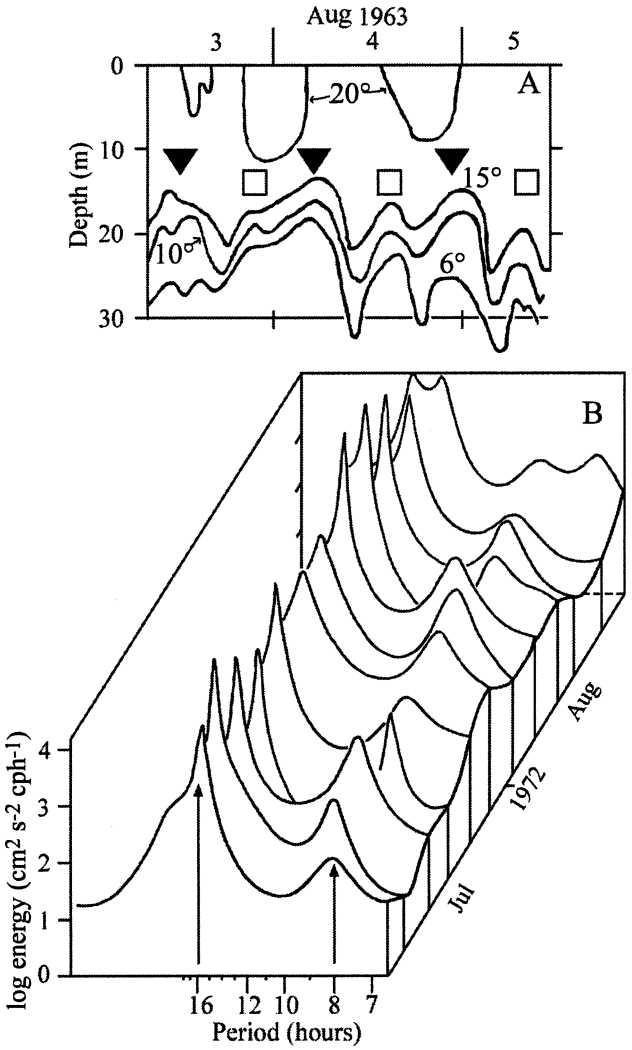


Fig. 5. (A) Depth oscillations of the 6°, 10°, and 15° isotherms at Lake Michigan anchor station M2, 03 to 05 August 1963 (adapted from Mortimer 2004); and (B) internal wave-energy spectra, Lake Ontario, July–August 1972, extracted from Marmorino and Mortimer (1978). Solid triangles and open squares in (A) mark inertial and half-inertial crests, respectively.

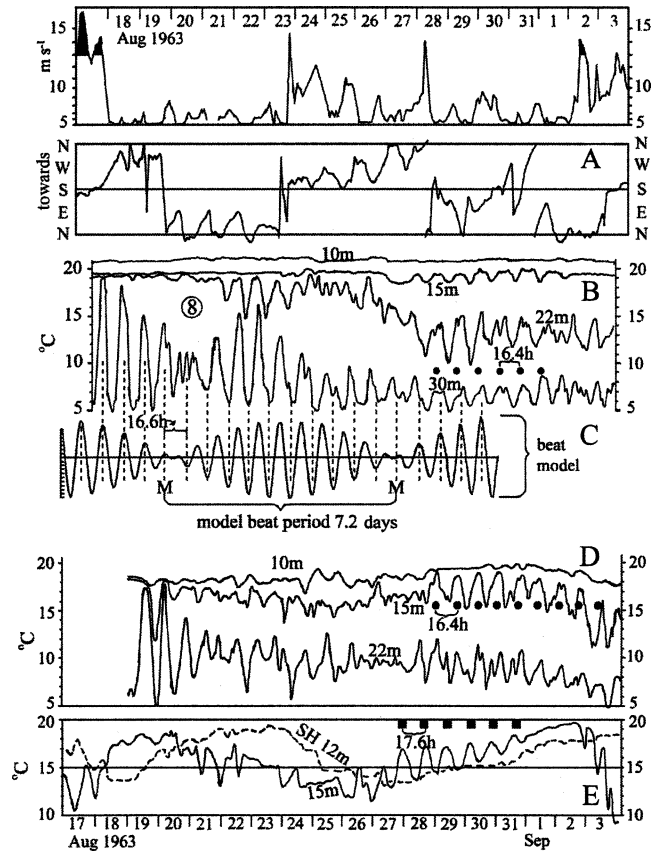


Fig. 6. Lake Michigan, 17 August to 03 September 1963 with data sources as for Fig. 4. (A) Midpoints of FWPCA 2-hourly envelopes of wind speed (on squared scale to simulate stress) and direction at Sta. 9; (B) temperature (°C) at 10-, 15-, 22-, and 30-m depth at Sta. 8; (C) beat pulsation model, fitted to 08 to 13 August portion of (B); (D) temperature (°C) at 10-, 15-, and 22-m depth at Sta. 9; and (E) temperature (°C) at 15-m depth at Sta. 11 and at 12-m depth (dashed line) at nearby South Haven water intake. Equally spaced vertical dashed lines and symbols indicate estimates of the mean oscillation (MO) periods.

oscillations 19–21 August were out of phase with those at Sta. 8. The same was true for the weaker oscillations 28 to 30 August, after the 28 August wind pulse. The probable explanation may be sought in the Fig. 2B model channel. This places Sta. 8 and 9 on opposite sides of and at different distances from the midchannel node, perhaps explaining their out-of-phase behavior and why the records from Sta. 8 show a distinct beat pattern, whereas those from Sta. 9 do not. Those differences emphasize the controlling influence of (i) amplitude differences between participating modes and of (ii) station location, relative to their nodal and antinodal positions.

Regrettably, I found no records for Sta. 10. The record for Sta. 11, 5 km from the east shore, was irregular except for the short Fig. 6E series of 17.6-h oscillations (presumably first mode dominant) after the 28 August wind pulse. The intake temperature from 12-m depth at nearby South Haven (dashed line) did not oscillate but followed the Sta. 11 general trend.

Figure 7 presents another example of the effectiveness of short, strong wind impulses as initiators of inertial oscillations. The impulse of 12 September was followed by two weeks of relative calm, during which beat patterns developed in both temperature and current records from Sta. 8. The temperature record there is the clearest example of a beat pulsation response yet seen in Lake Michigan. The 4-d spacings of the three minima M and the 15.8 h MO period, with half cycle phase changes at each minimum, identify (in Table 2) that beat pattern as a combination of the third and seventh modes. As in episodes in earlier figures, the MO period of the current oscillation was longer than that of the temperature oscillation. As explained earlier, this is a consequence of the relationship between mode wavelength and partition of kinetic and potential energy.

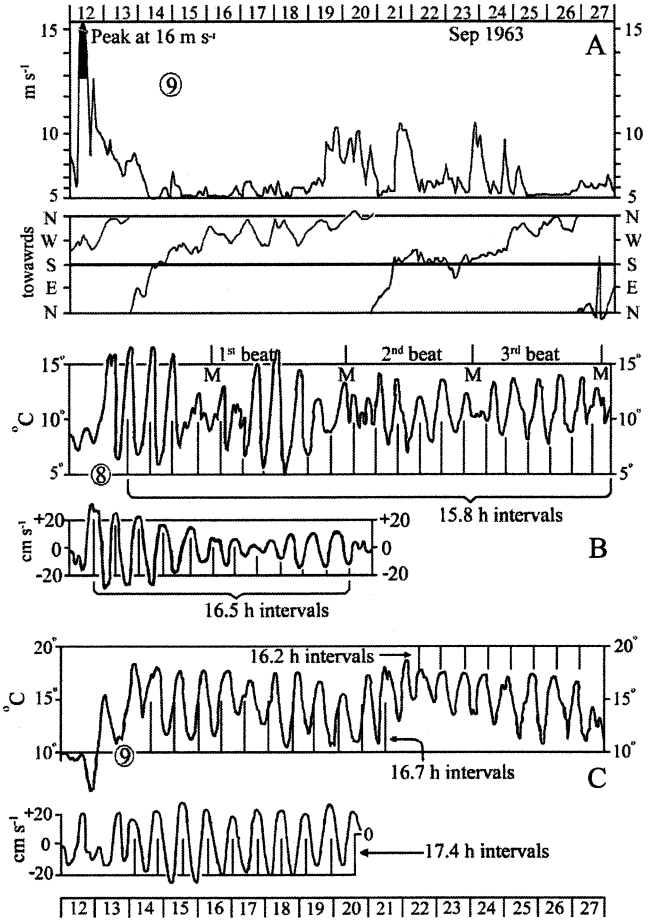


Fig. 7. Lake Michigan, 12 to 27 September 1963. (A) Midpoints of FWPCA 2-hourly envelopes of wind speed at Sta. 9 (squared scale to simulate stress) and direction; (B) temperature (°C) at 15-m depth at Sta. 8 (FWPCA 1967) and NS component of current (Malone 1972); (C) as for (B) but for Sta. 9. Equally spaced vertical lines estimate MO periods.

Again, as in Fig. 6, the beat pattern at Sta. 8 does not appear at Sta. 9, which (as Fig. 2B shows) was positioned close to the midlake node on the side opposite to that of Sta. 8. The first cycles of temperature oscillation at Sta. 8 and 9 (13–15 September) were out of phase. Thereafter, the phase differences steadily changed, because the MO period at Sta. 8 remained at 15.8 h, whereas that at Sta. 9 was longer (16.7 h changing to 16.2 h after 22 September). Evidently, these complexities invite investigation and again point to the influence of (i) station location relative to the nodal and antinodal positions and (ii) the amplitudes of participating modes.

*The International Field Year for the Great Lakes (IFYGL) in Lake Ontario 1972–1973*—Another large-scale deployment of current, wind and temperature recorders occurred during the International Field Year for the Great Lakes (IFYGL) during 1972 and the following winter. That campaign (Aubert and Richards 1981) was jointly operated by: the Canadian Meteorological Service; Canada Centre for Inland Waters (CCIW); the U.S. National Oceanic and

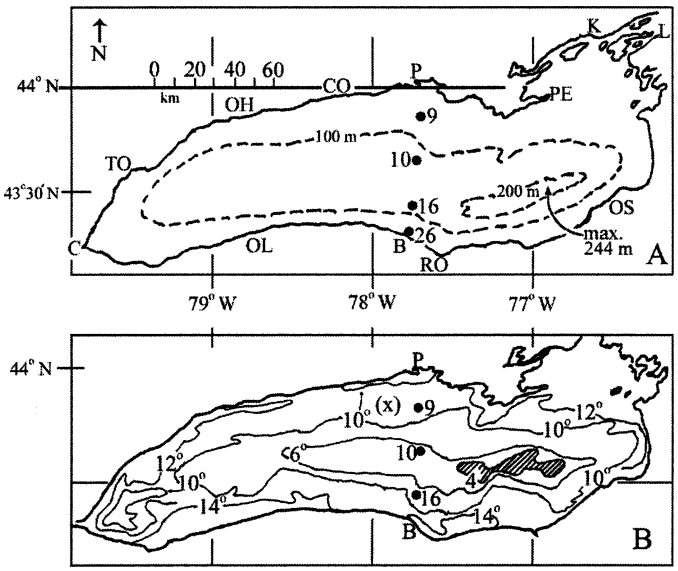


Fig. 8. Lake Ontario maps of (A) locations (solid circles) of 1972 recording stations here studied; and (B), surface temperature (°C) on 27 June 1972, redrawn from Irbe and Mills (1976). Within the hatched area, the surface temperature was <4°C. (A) Depth contours. Letters indicate place names: C, Canada Centre for Inland Waters; TO, Toronto; OH, Oshawa; CO, Cobourg; P, Presqu'ile; PE, Prince Edward Point; K, Kingston; L, St. Lawrence River Outflow; OS, Oswego; RO, Rochester; B, Braddock Point; OL, Olcott.

Atmospheric Administration (NOAA); and several university groups. Over 30 moored stations and instrumented towers were deployed. CCIW and NOAA vessels surveyed isotherm-depth variations by cruising to and fro across three transects (OL to OH, B to P, and OS to PE, Fig. 8A). All results were assembled in Boyce and Mortimer (1977). Attention here will be confined to Sta. 9, 10, 16, and (briefly) 26, spaced across the Braddock Point to Presque'ile (BP) transect (Fig. 8A). Illustrations, which now follow, are adapted from assemblages of figures in Marmorino and Mortimer (1978) and Mortimer (1980) prepared from the IFYGL data bank, now in NOAA archives, Ashville, North Carolina.

*Inertial episodes in Lake Ontario during winter and early spring*—As in Lake Michigan, the winter and summer inertial responses in Lake Ontario differed profoundly in several ways. Marmorino (1978) examined continuous current and temperature records at 15- and 75-m depths at the midlake Sta. 10 (Fig. 8) and at eight other Lake Ontario stations (12 km from shore and spaced 50 km apart) covering December 1972 to March 1973. Inertial oscillations were confined to currents and were seen only in "rare" episodes lasting 3 to 4 d between storms. They accounted for only up to 10% of the total current variance at Sta. 10. This is in contrast to the 50% seen in summer in that lake (Marmorino and Mortimer 1978).

The strongest winter inertial activity was seen (Marmorino 1978) during weak inverse stratification, 15 February to 15 March (near 0.5°C at 16 m and 2°C at 75 m). Spectral analysis of that and weaker episodes of inertial currents led

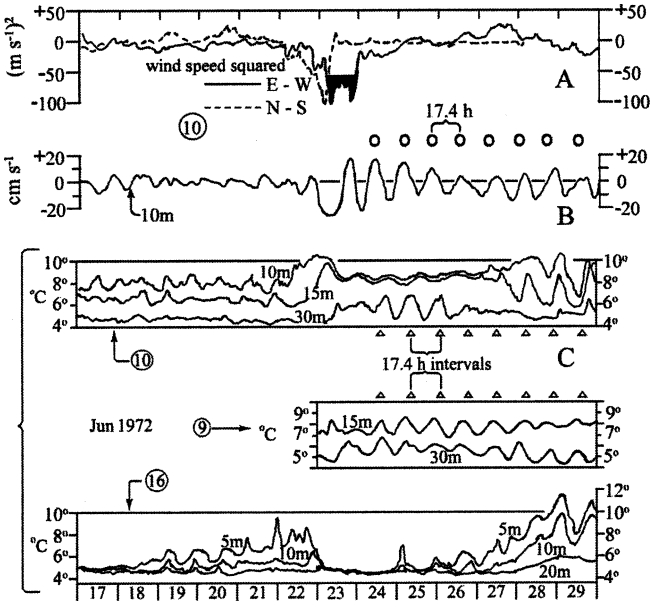


Fig. 9. Lake Ontario, 17 to 29 June 1972. Influence of a storm on stratification developing across the B-P transect. (A) EW and NS components of wind speed squared (simulating stress) at Sta. 10; (B) EW component of current at 10-m depth at Sta. 10; (C) temperature (°C) at various depths at Sta. 10, 9, and 16. Equally spaced symbols mark estimates of the mean oscillation (MO) periods during oscillatory episodes.

Marmorino to conclude, "the frequency of only the strongest inertial currents was close to the local theoretical value; otherwise, it was greater or less than that value." He attributed that small variation to Doppler interactions with other current systems.

The February–March episode at Sta. 10 ($T_{in}$ 17.38 h) is illustrated in Marmorino's (1978, fig. 12). My measurements on an enlargement of that figure confirm that the MO period throughout that set of episodes (17.4 h) did not vary by more than ±0.1 h from $T_{in}$. This is in contrast to the much greater and more variable reductions in period seen during summer stratification. During March, Marmorino observed inertial responses with features similar to the findings of Krauss (1972) in a model ocean consisting of a homogeneous upper (Ekman) layer and a continuously stratified lower layer. Inertial motions, generated by wind in the upper layer, transmitted energy downwards, producing waves of differing vertical modes in the lower layer, superposition of which led to beat interactions.

Because stratification is very weak in winter, in Lakes Ontario and Michigan, the inertial responses to wind are currents (kinetic energy) alone, circling with periods very close to $T_{in}$; and no Poincaré modes are seen. Stated in another way, with $c_i$ indistinguishable from zero, the periods of all Poincaré modes converge on $T_{in}$. The potential/kinetic energy ratio is also zero; and currents are the only inertial responses. Only when stratification returns, does that ratio become positive; and only when whole-basin stratification is established can Poincaré modes appear.

*Events leading to whole-basin stratification in Lake Ontario*—The 1972 season of thermal stratification began, as in most large temperate lakes, on the inshore side of a thermal front, which then moved progressively offshore into unstratified water (<4°C). On 23 May 1972, an airborne survey of surface temperature (Irbe and Mills 1976, not illustrated here) showed that Tower 26 (Fig. 8A) was on the inshore side of the front in thermally stratified water, whereas Sta. 10 and 16 were in water columns isothermal near 3°C. During the interval 17 to 24 May, strong regular current rotations were seen at Tower 26 (Mortimer 1977) with periods within 0.1 h of local inertial. No oscillations were then seen at Sta. 9, 10, or 16.

One month later (Fig. 9C, 22 June), stratification had become established at all three of those stations, but on 23 June was completely destroyed at Sta. 16 by sudden upwelling. This occurred during a strong southgoing then westgoing storm on 23 June, the aftermath of hurricane Agnes. At the same time at Sta. 10, in midlake, the storm mixed the upper water column down to below 15 m; and the initially weak current at 10-m depth was forced by the storm into strong regular oscillation (MO period 17.4 h). Similarly forced were temperature oscillations at Sta. 9 and 10, all with MO periods (17.4 h) indistinguishable from the local $T_{in}$ (17.38 h). Again, because whole-basin stratification was then not complete, cross-basin Poincaré modes could not yet develop.

After the storm had passed, stratification redeveloped at Sta. 16; but the 27 June surface temperature map (Fig. 8B) showed that a small central pool of unstratified (4°C) water (shown hatched) still remained near Sta. 10. Whole-basin stratification was, even then, not yet quite complete; and MO periods of both current *and* temperature oscillations all remained near $T_{in}$ at 17.4 h.

Whole-basin stratification was not completed until early July 1972. After a wind impulse on 15 July (not illustrated), Sta. 9, 10, and 16 showed current and temperature oscillations with respective MO periods of 17.2 and 17.0 h (Mortimer 1980), signifying that at least two Poincaré modes were active. The last line in Table 1 identifies that response as a dominance of the first mode, perhaps the first of the season.

*Beat pulsations and other inertial responses in Lake Ontario 1972 after establishment of whole-basin stratification*—As in Lake Michigan (Figs. 4 and 7), short strong wind action on Lake Ontario during the evening of 26 July (Fig. 10) evoked a short burst of circling current at Sta. 10 (MO period 16.4 h) and strong temperature oscillations at Sta. 10 and 16 (MO period 15.4 h). The phase relationship between Sta. 10 and 16 will be discussed in a later section. Here is noted only some evidence of a beat pulsation, aborted by the storm on 02 August.

Isotherm depth distributions across the BP transect, observed on repeated crossings, during 27 to 28 July are illustrated in later Figs. 14 to 16. They showed strong localized downwelling at the south end of the transect and diffuse upwelling in the northern third. The duration of that set of transect surveys is marked by a black bar in Fig. 10.

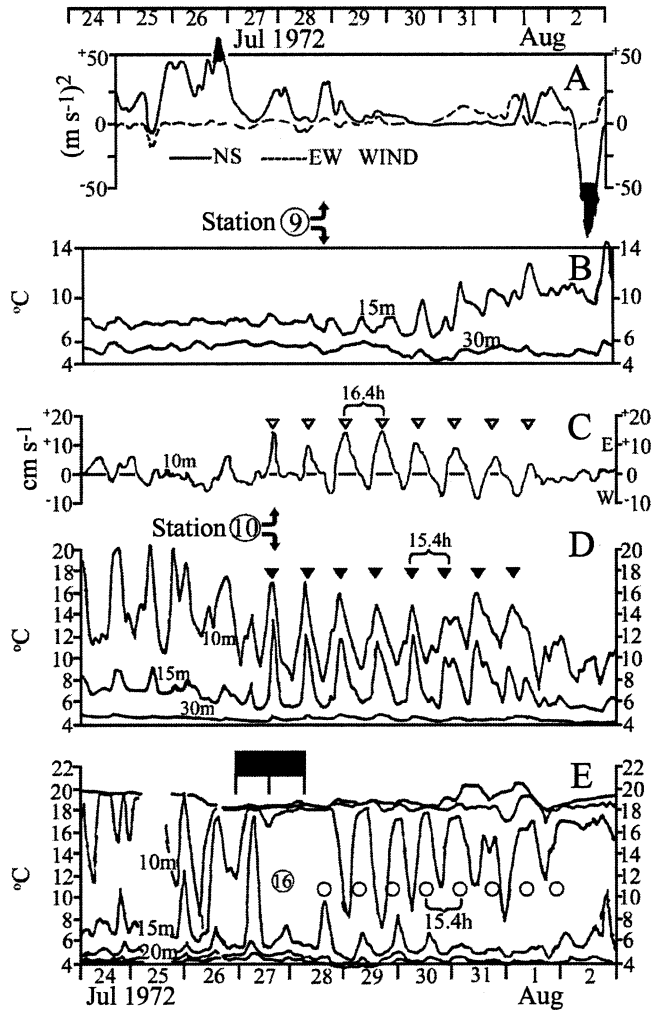


Fig. 10. Lake Ontario, 24 July and 02 August 1972, after establishment of cross-basin stratification. (A) EW and NS components of wind speed squared at Sta. 9; (B) temperature (°C) at 15- and 30-m depths at Sta. 9; (C) EW component of current at 10-m depth at Sta. 10; (D) temperature (°C) at 10-, 15-, and 30-m depth at Sta. 10; and (E) temperature (°C) at 5-, 10-, 15-, 20-, and 30-m depth at Sta. 16. Equally spaced symbols mark estimates of the mean oscillation (MO) period during oscillation episodes. The duration of the Fig. 15 and 16 transect plots are marked by a black bar, below which lines indicate the starts of transect run Nos. 10, 14, and 18.

Figure 11, which covers most of the 1972 stratified season, is a synoptic view of oscillatory responses to wind impulses. It facilitates the search for possible beat sequences. These can develop only if the wind impulse is followed by a long-enough interval of weak wind or calm. It appears from Fig. 11 that long calm spells after storms were less frequent in Lake Ontario in 1972 than in Lake Michigan during the 1963 stratified season. The only extensive beat sequence in Lake Ontario, showing the diagnostic phase-change at minima, was that seen after the storm on 09 August. The prelude and postlude to that storm are illustrated in Fig. 12 and its continuation, Fig. 13.

The short wind impulse on 04 August (Fig. 12A) generated current oscillation at Sta. 10 (Fig. 12B; MO period 17.0 h) and temperature oscillation at Sta. 10, 9, and 16 (Fig. 12C–E; MO periods all 16.8 h). Table 2 suggests that the 04–09 August response was the beginning of a first and third mode combination.

That response was, however, aborted by the 09 August strong eastgoing storm, which started a new and much longer beat response, permitted to evolve with a remarkably low dissipation rate during two weeks of relative calm that followed the storm. The MO period of Sta. 10 current oscillation (Fig. 13B) remained unchanged at 16.8 h from 10 to 27 August.

The temperature oscillations at Sta. 9 and 10 were irregular from 10 to 15 August, but thereafter (Fig. 13C,D) settled down to a regular 16.8 h periodicity, i.e. not distinguishable from the MO period of the current oscillation at Sta. 10. This is exceptional, because other inertial episodes, seen during full stratification in both Lakes Michigan and Ontario, usually display slight period differences between temperature and current oscillations, as described and explained earlier. The temperature record at Sta. 16, absent from 10 to 15 August, was too irregular thereafter (Fig. 13E) to assign an MO period.

The beat pulsation, started by the 09 August storm, was most clearly expressed in the current oscillation. The amplitude fell to minima M on 14 and 23 August, revealing a 9-d beat period. At both minima M of the current record (less clearly so in the temperature record) the oscillations changed phase by one half cycle.

The diagnostic MO phase change at each minimum M reveals, as in the Lake Michigan examples, the presence of a beat-pulsation, identified by its beat and MO periods in Table 2 as a combination of the first and third internal Poincaré modes, corresponding to an internal Merian celerity $c_i$ of 0.3 m $s^{-1}$. As pointed out in the footnote to Table 2, higher $c_i$ settings would have produced beat periods shorter than 9 d.

Figures 12 and 13 also reveal that the minima M in the Sta. 10 current record follow, by 1 or 2 d, the less distinct minima in temperature records. This may, again, be attributed to differences between participating modes in their partitions of kinetic and potential energy.

*Periodic release and radiation of internal surges from a downwelled front*—Contributions to the IFYGL campaign from the Center for Great Lakes Studies (University of Wisconsin-Milwaukee) included: Marmorino's earlier-described analysis (1978) of inertial motion in winter; the development of a depth-undulating temperature/pressure recorder (Fig. 14); and its operation on repeated tows across the BP (Fig. 8A) transect, complete results from which were assembled, with those from other transects, in Boyce and Mortimer (1977).

The BP tows revealed that the 09 August storm had caused strong downwelling along the south shore. During adjustment after the storm, internal surges emerged at 15-h intervals from the downwelled front and migrated northward across the basin. Their emergence coincided with (triggered by) the downswing of the oscillating thermocline

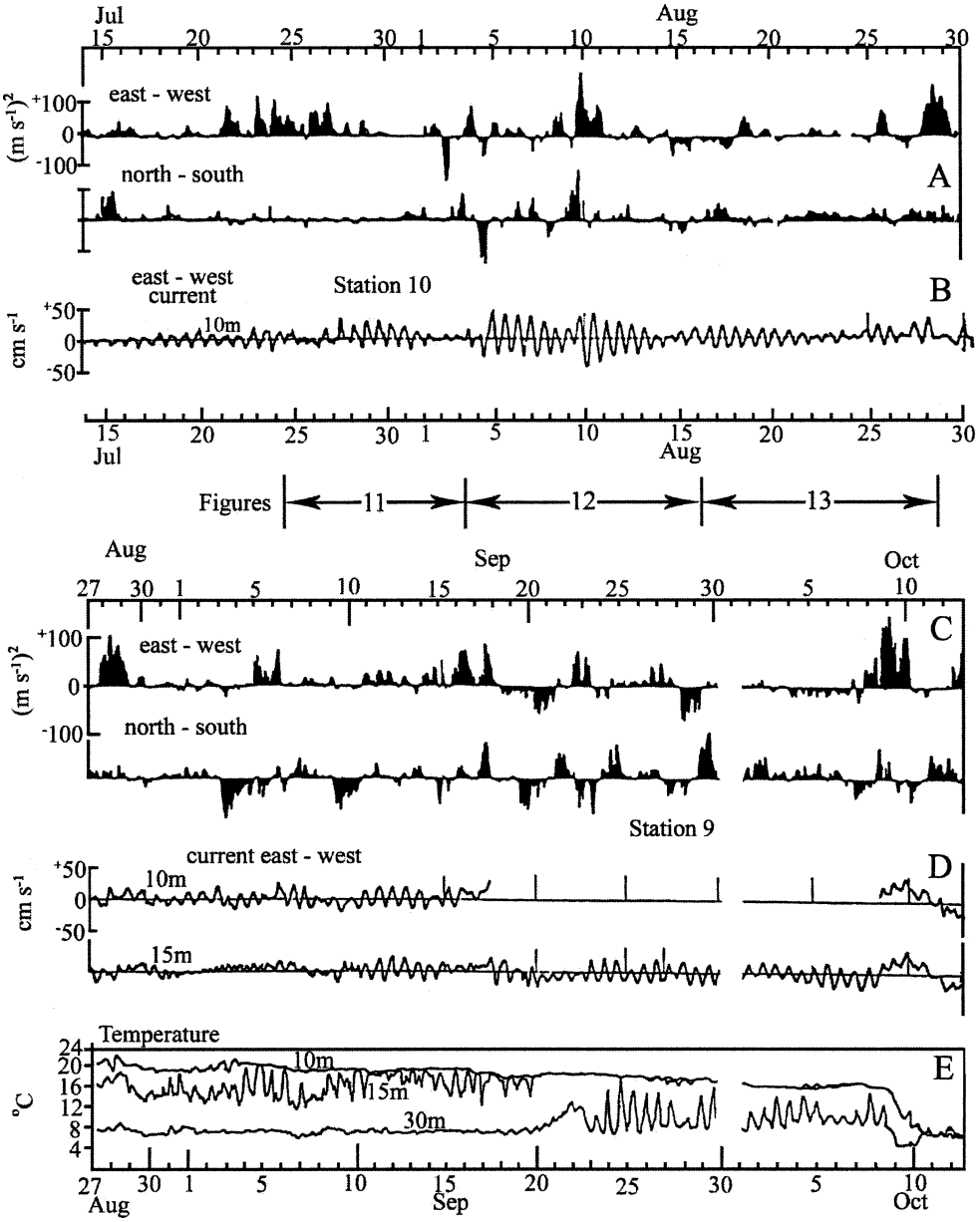


Fig. 11. Lake Ontario, 14 July to 12 October 1972, synopsis of a stratified season's responses to wind impulses (prepared by G. O. Marmorino for Marmorino and Mortimer 1978 and for Mortimer 1980). (A) EW and NS components of wind speed squared at Sta. 10, 14 July to 29 August; (B) EW component of current at 10-m depth at Sta. 10, 14 July to 29 August; (C) EW and NS components of wind speed squared at Sta. 9, 27 August to 12 October; (D) EW component of current at 10- and 15-m depth at Sta. 9, 27 August to 12 October; and (E) temperature (°C) at 10-, 15-, and 30-m depth at Sta. 9, 27 August to 12 October. Lines below (B) mark the durations of Figs. 10, 12, and 13.

(Mortimer and Cutchin 1974). On the basis of those findings, the phenomenon was modeled by Simons (1978) and illustrated by Gill (1982) as an example of a *geostrophic adjustment process*.

Another regular sequence of internal surge releases occurred after the earlier eastgoing storm on 26 July (Fig. 10). That storm started near midnight 25/26 July, decreased in strength around midday on 26 and reached its peak that evening, to fall to weak wind after midnight. Then a series of tows began, to-and-fro across the Braddock Point to Presqu'ile (BP) transect, using the depth-undulating temperature probe illustrated in Fig. 14. The first of the isotherm-depth plots, so obtained, is also illustrated in Fig. 14. It shows: a sharply defined downwelled front D about 7 km off Braddock Point; diffuse upwelling in northern quarter of the transect; and an internal surge at South, then encountered 35 km north of Braddock Point. The locations of recording Sta. 9, 10, and 16 are marked by circled numbers along the baseline of Fig. 14.

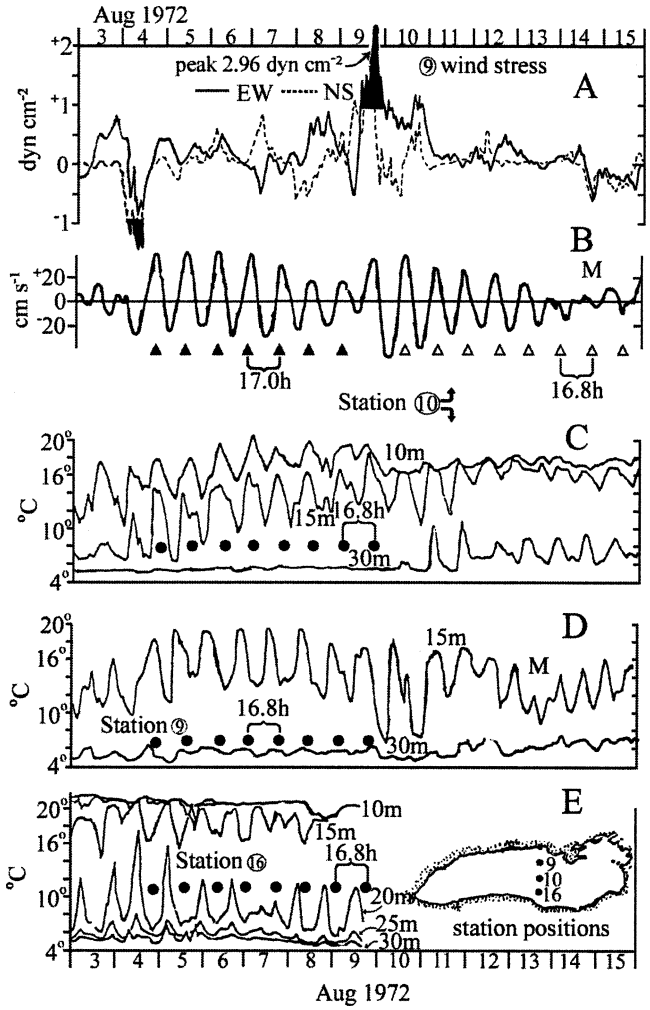


Fig. 12. Lake Ontario, 03 to 27 August 1972. (A) EW and NS components of wind stress on the water surface (Hamblin and Elder 1973). (B) NS component of current speed at 10-m depth at Sta. 10; (C) temperature (°C) at 10-, 15-, and 30-m depth at Sta. 10; (D) temperature (°C) at 15- and 30-m depth at Sta. 9; (E) temperature (°C) at 10-, 15-, 20-, 25-, and 30-m depth (10–16 August omitted) at Sta. 16. Equally spaced symbols estimate mean oscillation (MO) periods. M marks minima in the beat pulsations described in the text.

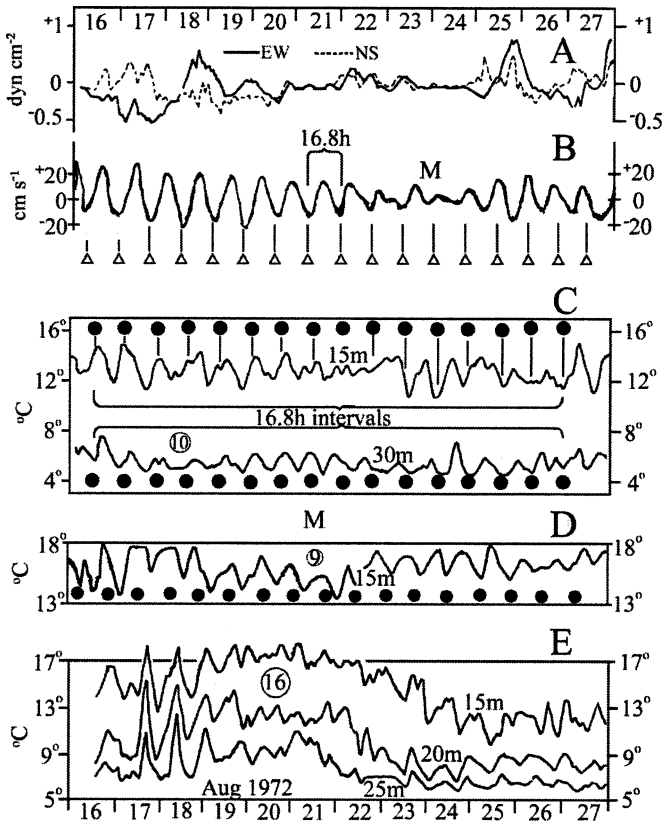


Fig. 13. Continuation of Fig. 12 (with temperature at some depths omitted); *see* Fig. 12 caption.

Arranged in a vertical stack in Fig. 15, the 10°C (midthermocline) isotherms from each transect are plotted to show the periodic releases of internal surges (shown hatched) from the southern downwelled front and their subsequent northward cross-basin progress.

Arranged on a time/distance plane in Fig. 16, the approximate transect tracks are shown by dashed lines; and all encounters with internal surges on those tracks are marked by solid circles. At top right in the figure, the encounters on Transect Nos. 10 and 11 are from a first surge release (not shown), which must have occurred near midday on 27 July during the lull in the storm (Fig. 10). Transect 10 also shows (top left) the start of the second front release at 01:00 h 27 July, also seen at D in Fig. 14. The third front release occurred 15 h later in Transect No. 14; and 15 h after that there was a weak indication (open circle at Transect 17) of a fourth front release.

The tracks of the surge encounters, spaced 15 h apart on the Fig. 16 time/distance plane, indicate a here-unexpectedly high mean speed of 2.2 km $h^{-1}$ or 61 cm $s^{-1}$, i.e. $\approx 2c_i$. The surge "tracks" in Fig. 16 are sinuous because, as Simons (1978) pointed out for the 09 August surge releases, the surges are migrating through fields of inertially circling currents, driven by the cross-basin Poincaré mode(s).

As noted earlier, Tables 1 and 2 and the observed 15.4 h MO for the temperature oscillations at 15-m depth on 27 July to 01 August in Fig. 10 point to a third and fifth mode combination, leading to an aborted beat pulsation. The clear out-of-phase relationship between those oscillations at Sta. 10 and 16 place the midlake node between those stations, probably near 30 km from Braddock Point (B). The contemporary temperature oscillation at 15-m depth at Sta. 9 is much smaller and establishes no clear phase relationship with Sta. 10. This suggests that Sta. 9 was near another node.

Significant is the coincidence of surge release from the front and the downswing there, every 15 h, of the third mode-dominated thermocline. A similar geostrophic adjustment, with periodic surge migration after downwelling, has not yet been seen but should be expected in Lake Michigan.

To summarize, this paper is confined to a description of internal Poincaré wave responses to wind forcing in the middle reaches of two basins of width order 100 km, in

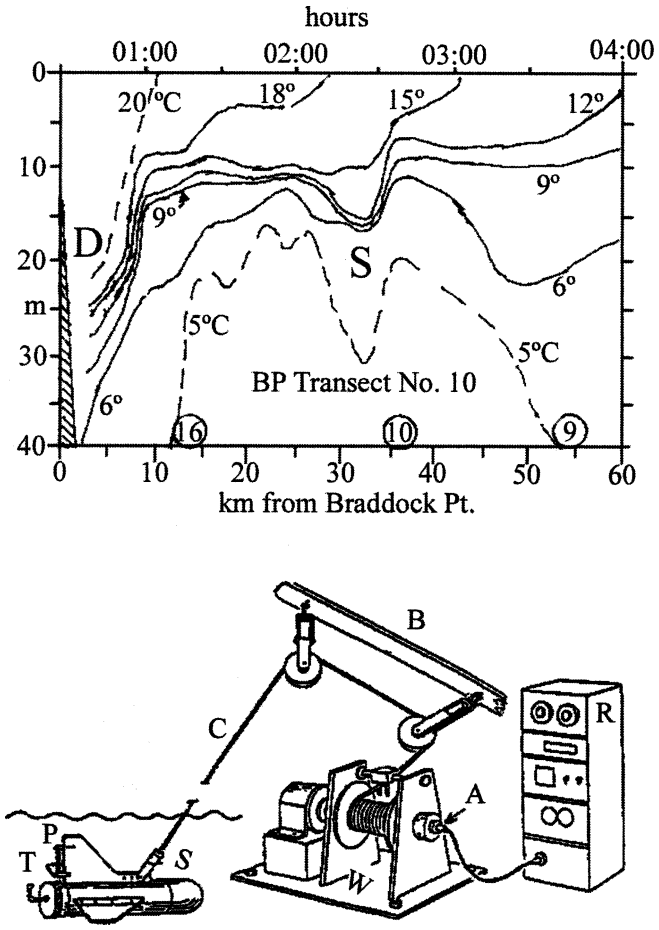


Fig. 14. Lake Ontario, depth distribution of temperature isotherms across the southern 60 km of the Braddock Point to Presqu'ile (BP) transect, 00:30 to 04:00 h GMT 27 July (adapted from Mortimer 1980) as measured by the depth-undulating probe, illustrated below. Displayed are the downwelled front D (created by the 25–26 July storm; *see Fig. 10*) and the internal surge South, migrating northward away from the front. Along the bottom scale (km from Braddock Point) are circled locations of Sta. 16, 10, and 9. Components of the probe, built by R. A. Scott and D. N. Baumgartner, are the temperature sensor (T), pressure/depth sensor (P), commutating swivel (S), winch axle (A), conductor cable (C), beam with sheaves (B), winch (W), and recorder (R).

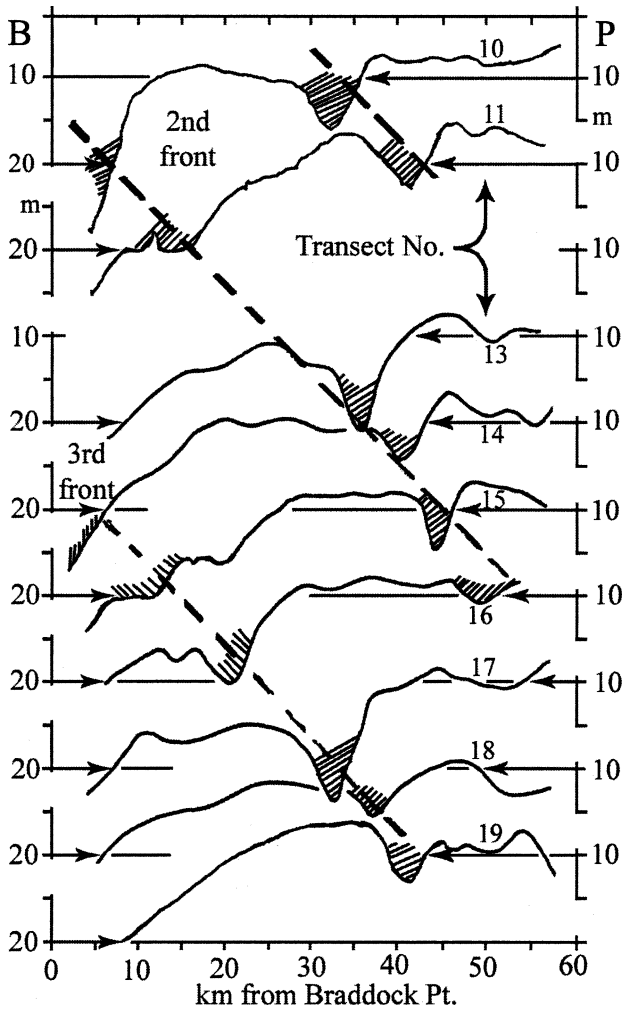


Fig. 15. Lake Ontario, 00:30 h on 27 July 1972 to 12:00 h on 28 July 1972, depths of 10°C (midthermocline) isotherms measured by the Fig. 14 probe towed across BP transects Nos. 10 to 19 (transect No. 12 was incomplete and is here omitted). The duration of this set of transects is marked by a black bar in Fig. 10. To display the successive northward migration of internal surges (shown hatched), the individual isotherm depth traces are stacked with vertical separation to simulate a timescale.

which internal Kelvin waves are trapped to within 20 km of the shores. Therefore, treatments of Kelvin waves and their interactions with vorticity (topographic Rossby) waves in variable-depth basins are here omitted. Vorticity waves were recorded, as whole-basin phenomena in Lake Michigan, by Saylor et al. (1980); and their interactions with internal Kelvin waves in that Lake were described by Beletsky et al. (1997) and, in Lake Ontario, by Simons (1980). To provide a combined picture of these wave classes, their responses to wind action and their interactions, call for answers to the following questions: (1) What, in basins of this size order, are the characteristics of baroclinic Poincaré modes when extended from the middle reaches (treated here) to the whole basin? (2) What are their interactions with Kelvin and vorticity waves? (3) Which features characterize geostrophic adjustments when wind starts, continues and stops? (4) What determines the here-observed high propagation speed of the poststorm internal surges in Lake Ontario (Figs. 14 to 16); and do similar surges occur in Lake Michigan? (5) What factors determine which of the internal Poincaré cross-basin nodes are excited and how strongly?

The search for the answers will be aided by: (i) specifically focused in-lake and on-lake measurements, paying closer attention than before to the structure and time-history of the forcing wind field, to its strength distribution over the lake surface and to its duration, periodicity and curl; (ii) further mining of the archived databanks listed below; (iii) numerical modeling; and (iv) more advanced analytical modeling.

Tool (iii) has successfully simulated observed baroclinic Kelvin waves and illustrated their structure and behavior in Lake Michigan (Beletsky et al. 1997) and in Lake of

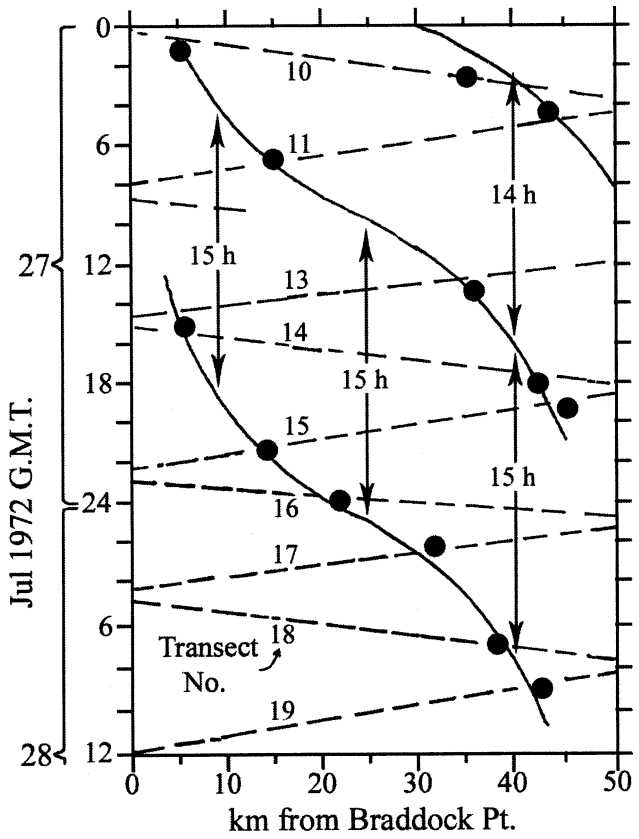


Fig. 16. Approximate tracks of the Fig. 15 transects are here plotted as straight, dashed lines on a distance/time plane; and encounters with migrating surges are marked as solid circles. The sinuosity of the paths of their cross-basin migrations are explained in the text.

Geneva (Lemmin et al. 2005). Antenucci and Imberger (2001, 2003) used tool (iv) to demonstrate the baroclinic responses of Kelvin and Poincaré waves to periodic (diurnal) wind forcing on Lake Kinneret. Added to that advance is Stocker and Imberger's (2003) modeling of dispersion and energy partitioning in rotating stratified circular model basins. A two-layered laboratory version of such models (diameter 97 cm, depth 50 cm) was used by Wake et al. (2004) to study responses to a steplike discontinuity imposed and then released on the density interface.

The following data archives, of evident value in this paper, can also help in the search for answers to the above and further questions. Sources are: (1) Wind and multi-depth current records, plotted by Mehr (1965) for the FWPCA format of Fig. 1, from the whole–Lake Michigan 1962 campaign, deposited in the Golda Meir Library Archives, University of Wisconsin, Milwaukee. (2) All records from the 1972 IFYGL campaign on Lake Ontario, archived in NOAA's U.S. National Climatic Data Center, Ashville, North Carolina. (3) NOAA's Great Lakes Environmental Research Laboratory, Ann Arbor, Michigan, retains wind, current and temperature records from various campaigns, many reports on which are referenced in Mortimer (2004), to which the present paper is an appendix.

## References


Allender, J. H. 1977. Comparisons of model and observed currents in Lake Michigan. J. Phys. Oceanogr. **71:** 711–732.

Antenucci, I. P., and J. Imberger. 2001. Energetics of long internal gravity waves in large lakes. Limnol. Oceanogr. **46:** 1760–1773.

———. 2003. The seasonal evolution of wind/internal wave resonance in Lake Kinneret. Limnol. Oceanogr. **48:** 2055–2061.

Aubert, E. J., and T. L. Richards [eds.]. 1981. International Field Year for the Great Lakes (IFYGL) 1972. NOAA, Great Lakes Environmental Research Laboratory.

Beletsky, D., W. P. O'Connor, D. J. Schwab, and D. E. Dietrich. 1997. Numerical simulation of internal Kelvin waves and coastal upwelling fronts. J. Phys. Oceanogr. **27:** 197–215.

Boyce, F. M., and C. H. Mortimer. 1977. IFYGL temperature transects, Lake Ontario 1972. Environment Canada, Inland Waters Directorate Technical Bulletin 100.

FWPCA (Federal Water Pollution Control Administration). 1967. Lake currents: Water quality investigations, Lake Michigan basin. Technical report. FWPCA.

Gill, A. E. 1982. Atmosphere and ocean dynamics. Academic.

Hamblin, P. F., and F. C. Elder. 1973. A preliminary investigation of the wind stress field over Lake Ontario, p. 723–734. *In* Proceedings of the 16th Great Lakes Conference. Publication of the Great Lakes Research Division, Univ. Michigan.

Irbe, J. G., and R. J. Mills. 1976. Aerial surveys of Lake Ontario water temperature and description of regional weather conditions during IFYGL, January 1972 to March 1973. Atmosphere Environment Report CL I 76. Environment Canada.

Krauss, W. 1972. Wind-generated internal waves and inertial period motions. Deutsche Hydrogr. Z. **25:** 241–250.

Lemmin, U., C. H. Mortimer, and E. Bäuerle. 2005. Internal seiche dynamics in Lake Geneva. Limnol. Oceanogr. **50:** 207–216.

Malone, F. D. 1968. Analysis of current measurements in Lake Michigan. J. Geophys. Res. **73:** 7065–7081.

———. 1972. A numerical model of the wind-driven summer circulation in Lake Michigan. Ph.D. thesis, Dept of Oceanography, Engineering Science, New York Univ.

Marmorino, G. O. 1978. Inertial currents in Lake Ontario, Winter 1972–3. IFYGL. J. Phys. Oceanogr. **8:** 1104–1120.

———, and C. H. Mortimer. 1978. Internal waves observed in Lake Ontario, during the International Field Year for the Great Lakes (IFYGL) 1972. II. Spectral analysis and modal decomposition. Special Report 33. Center for Great Lakes Studies, Univ. Wisconsin–Milwaukee.

McCormick, M. J., R. L. Pickett, and G. S. Miller. 1991. A field evaluation of new satellite-tracked buoys: LORAN-C position recording and a Sonobuoy type drifter. Mar. Technol. J. **254:** 29–33.

Mehr, E. 1965. Computer processing of lake data 1963–64. Report of the Department of Oceanographic Engineering Science, New York Univ.

Mortimer, C. H. 1963. Frontiers in physical limnology with particular references to long waves in rotating basins, p. 9–24. *In* Proceedings of the 6th Conference on Great Lakes Research, Univ. Michigan (Ann Arbor). Publication 10. Great Lakes Research Division.

———. 1968. Internal waves and associated currents observed in Lake Michigan during the summer of 1963. Special Report 1. Univ. Wisconsin–Milwaukee, Center for Great Lakes Studies.

———. 1977. Internal waves observed in Lake Ontario during IFYGL 1972. Special Report 32. Univ. Wisconsin–Milwaukee, Center for Great Lakes Studies.

———. 1980. Inertial motion and related internal waves in Lake Michigan and Lake Ontario. Special Report 37. Univ. Wisconsin–Milwaukee, Center for Great Lakes Studies.

———. 2004. Lake Michigan in motion: Responses of an inland sea to weather, earth-spin and human activities. Univ. of Wisconsin Press.

———, and D. L. Cutchin. 1974. The internal wave response of the Lake Ontario thermocline to the passage of a storm 9–10 August 1972, p. 129–145. *In* American Geophysics Union Proceedings, 55th Annual Meeting, IFYGL Symposium. American Geophysics Union.

Platzman, G. W. 1971. Ocean tides and related waves. Am. Math. Soc. Lectures Appl. Math. **14:** 239–291.

———. 1972. Two-dimensional free oscillations in natural basins. J. Phys. Oceanogr. **2:** 117–138.

Poincaré, H. 1910. Théorie des marées: Leçons de mechanique céleste. V. 3. Gauthier-Villars.

Pollard, T. T., and R. C. Millard. 1970. Comparison between observed and simulated wind-generated inertial oscillations. Deep-Sea Res. **17:** 813–821.

Rossby, C.-G. A. 1937, 1938. On the mutual adjustment of pressure and velocity distributions in certain simple current systems. J. Mar. Res. **1:** 15–28, 239–263.

Saylor, J. H., C. K. Huane, and R. O. Reid. 1980. Vortex modes in southern Lake Michigan. J. Phys. Oceanogr. **10:** 1814–1823.

Schwab, D. J. 1977. Internal free oscillations in Lake Ontario. Limnol. Oceanogr. **28:** 700–708.

Simons, T. J. 1978. Generation and propagation of downwelled fronts. J. Phys. Oceanogr. **8:** 571–581.

———. 1980. Circulation models of lakes and seas. Can. Bull. Fish. Aquat. Sci. 203.

Stocker, R., and J. Imberger. 2003. Energy partitioning and horizontal dispersion in a stratified rotating lake. J. Phys. Oceanogr. **33:** 512–529.

Verber, J. L. 1963. Currents in southern Lake Michigan. Special Report LM 12. U.S. Department of Health, Great Lakes–Illinois River Basins Project.

———. 1964. The detection of rotary currents and internal waves in Lake Michigan. Proc. 7th. Conf. Great Lakes Res. Univ. Michigan Great Lakes Res. Div. **11:** 382–389.

———. 1966. Inertial currents in the Great Lakes. Univ. Michigan Great Lakes Res. Div. Publ. **14:** 375–379.

Wake, G. W., G. N. Ivey, J. Imberger, R. MacDonald, and R. Stocker. 2004. Baroclinic geostrophic adjustment in a rotating circular basin. J. Fluid Mech. **515:** 63–86.

*Received: 14 July 2005*
*Accepted: 5 April 2006*
*Amended: 5 April 2006*